NAVAL AIR WARFARE CENTER AIRCRAFT DIVISION
PATUXENT RIVER, MARYLAND

TECHNICAL REPORT

REPORT NO: NAWCADPAX--99-38-TR

MODELING OF PULSED THERMOGRAPHY IN ANISOTROPIC MEDIA

by

I. Perez
P. Kulowitch
W. Davis

7 May 1999

Aerospace Materials Division
Naval Air Warfare Center Aircraft Division
Patuxent River, Maryland

19990809 023

DTIC QUALITY INSPECTED 4

DEPARTMENT OF THE NAVY
NAVAL AIR WARFARE CENTER AIRCRAFT DIVISION
PATUXENT RIVER, MARYLAND

NAWCADPAX--99-38-TR
7 May 1999

RELEASED BY:

William Frazier signature   4/15/99

WILLIAM E. FRAZIER / DATE
Head, Metals and Ceramics Branch

Dale Moore signature

DALE MOORE / DATE
Director, Materials Competency
Naval Air Warfare Center Aircraft Division

REPORT DOCUMENTATION PAGE			Form Approved OMB No. 0704-0188

1. AGENCY USE ONLY (Leave Blank)	2. REPORT DATE 7 May 1999	3. REPORT TYPE AND DATES COVERED Technical Report

4. TITLE AND SUBTITLE

Modeling of Pulsed Thermography in Anisotropic Media

5. FUNDING NUMBERS

6. AUTHOR(S)

I. Perez
P. Kulowitch
W. Davis

7. PERFORMING ORGANIZATION NAMES(S) AND ADDRESS(ES)

Naval Air Warfare Center Aircraft Division
22347 Cedar Point Road Unit #6
Patuxent River, Maryland 20670-1161

8. PERFORMING ORGANIZATION REPORT NUMBER

NAWCADPAX--99-38-TR

9. SPONSORING / MONITORING AGENCY NAME(S) AND ADDRESS(ES)

Naval Air Systems Command
47123 Buse Road Unit IPT
Patuxent River, Maryland 20670-1547

10. SPONSORING / MONITORING AGENCY REPORT NUMBER

11. SUPPLEMENTARY NOTES

12a. DISTRIBUTION / AVAILABILITY STATEMENT

Approved for public release; distribution is unlimited.

12b. DISTRIBUTION CODE

13. ABSTRACT (Maximum 200 words)

Thermography is increasingly being used as an NDE tool to detect damage (corrosion, delamination, water incursion) in materials. Many empirical results have been collected over the years that allow the operator to get a "feel" for the extent of the problem. No simple models exist that provide quantitative results. Finite element analysis is done but is laborious and does not provide simple relationships which can be utilized for quantitative analysis of real world problems. In this report, we have performed a series of experiments where we vary many of the key parameters and perform simple thermographic modeling to find useful mathematical relationships.

14. SUBJECT TERMS

Thermography
Anisotropic Media

15. NUMBER OF PAGES

21

16. PRICE CODE

17. SECURITY CLASSIFICATION OF REPORT	18. SECURITY CLASSIFICATION OF THIS PAGE	19. SECURITY CLASSIFICATION OF ABSTRACT	20. LIMITATION OF ABSTRACT
Unclassified	Unclassified	Unclassified	SAR

ABSTRACT

Thermography is increasingly being used as an NDE tool to detect damage (corrosion, delamination, water incursion) in materials. Many empirical results have been collected over the years that allow the operator to get a "feel" for the extent of the problem. No simple models exist that provide quantitative results. Finite element analysis is done but is laborious and does not provide simple relationships which can be utilized for quantitative analysis of real world problems. In this report, we have performed a series of experiments where we vary many of the key parameters and perform simple thermographic modeling to find useful mathematical relationships.

ACKNOWLEDGMENT

CONTENTS

SUMMARY

This report describes the results of a study that was conducted to determine the effects of key experimental parameters (such as the amount of energy deposited, the panel thickness, the depth of the discontinuity, the normal thermal conductance, and the lateral thermal conductance) on the peak thermal contrast. For that purpose, a panels with various flat bottom holes was fabricated. Different amounts of heat were deposited on the surface of the panel and thermographic data were gathered. A simple model was developed which takes into account lateral heat conduction, anisotropic thermal conductivity, thickness, flaw size, density, and pulse duration. The final model provides a simple, yet accurate, description of the time dependence of the thermal contrast.

INTRODUCTION

As active thermography continues to gain acceptance as an NDE tool for both in-service and manufacturing applications, the need for robust physical models of the process increases. Although the sophistication of both analytical and numerical modeling efforts has increased considerably[1,2,3], development of a 3-dimensional model for anisotropic media is still a formidable task.

In a previous paper[4], a simple model was developed (referred to as Model I) to describe the surface temperature evolution of a 1/8 in. thick aluminum panel with fixed 1 in. diameter flat bottom holes of different depth in response to a short pulse of radiant energy. That model correctly described the temporal behavior of all 1 in. flat bottom holes. To further validate Model I, a new panel was fabricated (figure 1) that contained flat bottom holes of different diameters and different depths. After careful analysis of the data, it was found that Model I could not adequately account for the new experimental results. In this report, a new model is introduced that accurately describes the experimental data. The main difference between the models is the way in which thermal conductance is treated. In Model I, the thermal conductance was approximated by an effective contact conductance ($K=k_c \cdot A$ where k_c is a contact conductivity and A is the cross sectional area). In the new model, the thermal conductance is approximated by an effective thermal conductivity ($K=k \cdot A/l$ where k is the thermal conductivity and l is a characteristic length).
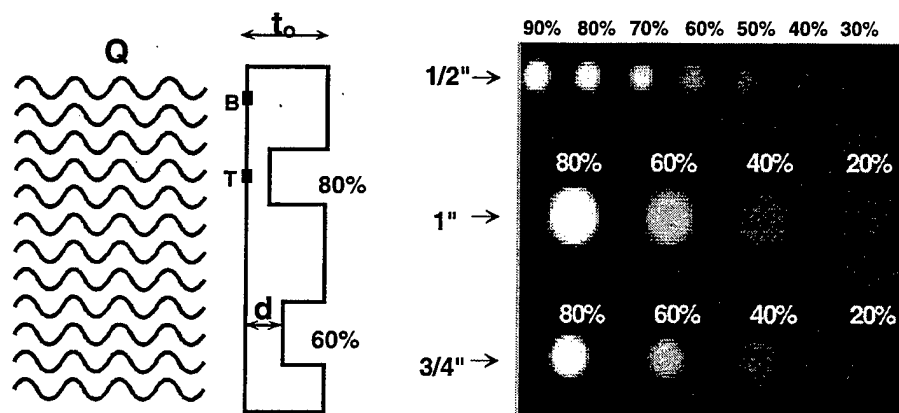
Figure 1: The figure on the left shows a 1/8 in. thick aluminum Al -7075 panel with flat bottom holes of 1, 3/4, and 1/2 in. diameters and various depths. The figure on the right shows a quasi-isotropic 1/8 in. thick graphite/epoxy composite with four flat bottom holes of 1/4 in. diameter and various depths.

EXPERIMENTAL PROCEDURE

The test sample was imaged using a liquid nitrogen cooled Amber Engineering 4128 InSb focal plane array (128 x 128) camera with silicon optics operating in the 3 - 5 micron spectral range. The samples were thermally excited with a pair of xenon arc lamps, each one powered by a 5 KJoule capacitor bank with a 10 msec discharge time.

The material used in this study was a 1/8 in. thick aluminum panel with various 1, 3/4, and 1/2 in. diameter flat bottom holes drilled at depths ranging from 25 to 100 mil in steps of 25 mil as shown in figure 1. The center to center distance between flat bottom holes was set to at least two diameters to minimize hole proximity effects. The arc lamps were positioned to produce a uniform distribution of heat over the sample surface. The distance from the arc lamps to the sample was approximately 14 in. The distance from the camera to the samples was approximately 22 in. The data acquisition rate was 43 frames/sec and a total of 100 frames were collected for each experiment. Figure 1 (left) shows a drawing with the key parameters used in the study and model. The parameter "Q" represents the amount of energy deposited on the surface of the sample per unit area. The parameters "t_o" and "d" represent the thickness of the panel and the distance from the surface of the panel to the defect (the words "defect" and "flat bottom hole" are used interchangeably in this report), respectively. The points "T" (just above a defect site) and "B" (far from any defect) are the points over the surface of the sample that where used to calculate the contrast. The quantities 80% and 60% represent the amount of material removed as a result of the drilling process. Figure 1 (right) shows an actual frame taken shortly after the flash pulse. The white areas in the image photo represent the flat bottom holes that tend to remain hotter than the background material since they are thinner.

RESULTS AND DISCUSSION

Data acquisition was initiated a few frames before the flash discharge in order to obtain a baseline amplitude value for the sample surface. The camera frame rate was set to 43 Hz and acquisition duration was 2.5 sec, so that 12-bit digital data were captured for the entire thermal cycle (from room temperature to final equilibrium temperature). Figure 2 shows the entire thermal history of two points on the surface of the panel. The curve labeled "defect" was taken from a point directly above and in the center of the flat bottom hole with 80% of material removed and it was referred as "T" in figure 1. This curve characterizes the thermal evolution of a typical damage site. The curve labeled "reference" refers to a point far away from any flat bottom hole and characterizes the thermal history of an undamaged site. Unlike the defect curve, the thermal history of the "reference" point does not decay monotonically, since there is a small increase in temperature in the reference curve at later times due to proximity effects. Both the "reference" and "defect" curves exhibit extremely elevated temperatures at early times. This is an artifact produced by reflection of the initial flash off of the sample and into the camera. It normally disappears when calculating the contrast curve.
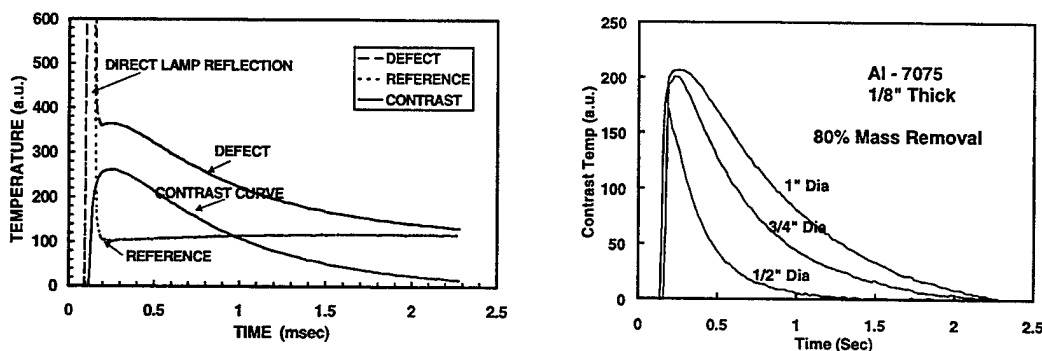

Figure 2: (Left) Raw data showing defect and reference points and the resulting contrast curve (defect – reference). (Right) Typical contrast curves for various flat bottom holes.

The difference between the "reference" and "defect" curves is termed the "thermal contrast" curve, indicated with a solid black line in figure 2 (left). Thermal contrast curves start and end with zero temperature since the initial and final equilibrium temperatures are uniform throughout the entire panel. Figure 2 (right) shows contrast curves for three flat bottom holes with 1, 3/4, and 1/2 in. diameters and 25 mil from the surface. It is clear from this figure that, although the distance from the panel surface to the defect is the same for the three holes, the peak contrast temperatures and times and the overall shape of the curves are significantly different. It will be shown later on in this report that these differences can be modeled if lateral heat effects are taken into account. Figure 3 (left) shows the peak contrast temperatures for all flat bottom holes in the panel. The contrast of the 1 and 3/4 in. diameter holes almost overlap for all defect depths. However, the contrast for the 1/2 in. diameter holes diameter is smaller than for the larger holes.
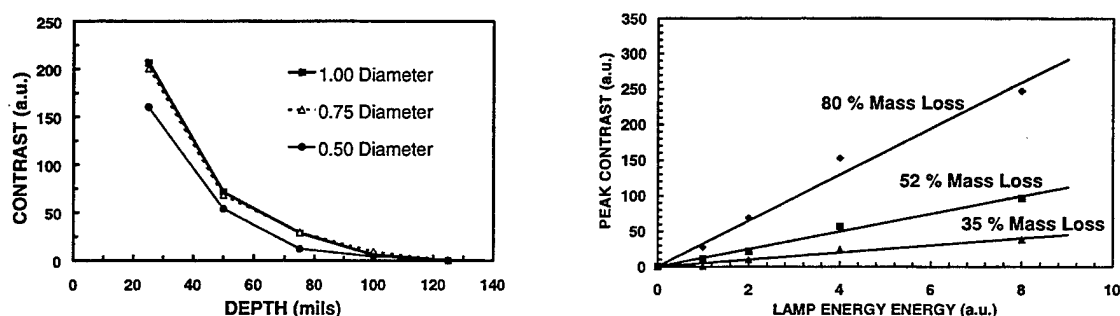
Figure 3: (Left) Peak contrast is plotted as a function of the amount of material removed. (Right) The relation between the "peak contrast" and the amount of heat deposited in the surface of the material is shown for three different defects.

An additional set of experiments was performed, increased to study the relationship between peak thermal contrast and amount of energy delivered to the sample surface. Figure 3 (right) shows the results of this experiment for the 1 in. flat bottom holes. The amount of energy deposited on the surface of the panel was controlled by changing the amount of charge stored in the capacitor banks. Four different settings were used which produced energy levels in the following amounts: $Q=1$, $Q=2$, $Q=4$, and $Q=8$, where Q represents the amount of energy deposited per unit area (the energy is expressed in arbitrary units). From figure 3 (right) it is clear that, for any given defect, as the energy deposited on the surface increases, the peak temperature contrast increases in linear proportion.

CALORIMETRIC MODEL (ZEROTH ORDER APPROXIMATION)

A simple theoretical model (zeroth order approximation) was introduced in our previous work[4]. Despite the fact that it was based in equilibrium thermodynamics and that no lateral heat effects were assumed, it correctly accounted for most of the observed experimental behavior of pulsed thermography. Figure 4 shows a schematic representation of the model. Drilled and undrilled regions are defined in the model, and it is assumed that no lateral energy flows between these regions. In the next section, a more refined model that takes lateral heat transfer effects into account will be derived.
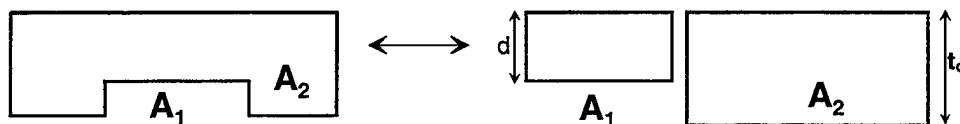

Figure 4: This figure shows a schematic representation of the zero lateral flow assumption used in the model.

From simple calorimetric arguments, it can be established that $q_1 = m_1 c T_1$ and $q_2 = m_2 c T_2$, where q_1, m_1, and T_1 are the energy deposited on block 1, the mass of block 1, and the final temperature of block 1 (similar definitions hold for block 2). The initial temperature of the panel can be assumed to be 0 deg. The mass can be written in terms of the density as $m_1 = \rho A_1 d$ and

$m_2 = \rho\, A_2\, t_o$. If it is assumed that the energy deposited on the surface of the panel per unit area is constant, i.e., $q_1/A_1 = q_2/A_2 = Q$, then the final equilibrium temperature difference (or thermal contrast) between both blocks $T_1 - T_2 = \Delta T$ will be

$$\Delta T = \frac{Q}{\rho c}\left(\frac{1}{d} - \frac{1}{t_o}\right)$$

(1)

This equation correctly accounts for most of the observed experimental behavior of pulsed thermography, i.e.,

1. The contrast temperature (ΔT) increases linearly with the amount of energy deposited per unit area (Q).
2. The higher the specific heat-density of a material ($\rho c \uparrow$) the smaller the contrast temperature becomes ($\Delta T \downarrow$).
3. The closer the defect is to the surface ($d \rightarrow 0$) the larger that the contrast temperature becomes ($\Delta T \rightarrow \infty$).
4. As the defect depth approaches the panel thickness ($d \rightarrow t_o$) the contrast temperature vanishes ($\Delta T \rightarrow 0$).
5. For a given defect depth d, the thicker the panel ($t_o \rightarrow \infty$) the larger the contrast temperature ($\Delta T \rightarrow Q/\rho c d$).

CALORIMETRIC MODEL (FIRST ORDER APPROXIMATION)

The previous model can be modified to allow for lateral heat flow effects. For the most general case, in this extension of the model, we assume that the in-plane and out-of-plane thermal conductivities are different. A "poor man's finite element approximation" (i.e., three elements only) will be used, but all the elements will be thermally interconnected. Figure 5 shows a schematic representation of the heat flow model.
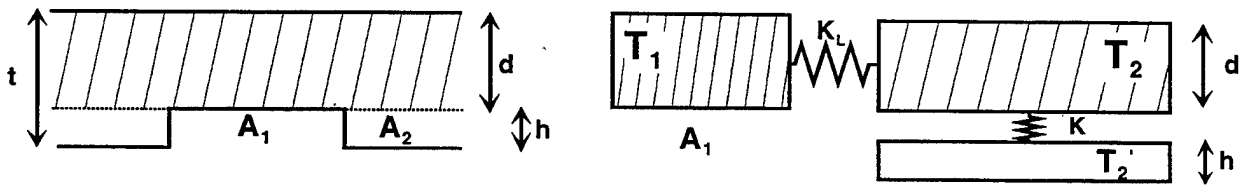

Figure 5: This figure shows the building blocks of the simple calorimetric model.

In this model, it will be assumed that all the energy of the heat pulse is absorbed in a layer of thickness "d". This layer corresponds to the material above the defect and is represented by the hatched region in figure 5. As a result of this heating process, the initial temperature of this layer "T_o" can be derived from simple calorimetric argument from $Q = \rho \cdot c \cdot d \cdot T_o$ where it is assumed that the temperature of the panel before the heat pulse was 0 deg. The total thickness of the panel is given by $t_o = d + h$ where h represents the amount of material under the defect. We assume that the in-plane material properties are isotropic, but different from the out-of-plane properties. The quantities K and K_L are the normal and lateral thermal conductance, respectively. These quantities can be expressed in terms of the in-plane and out-of-plane thermal conductivities of the panel as

$$K = k \cdot A_1 / (d + h)$$
$$K_L = k_L \cdot A_d / R \tag{2}$$

where "k" is the normal (out-of-plane) thermal conductivity of the material (in this case aluminum), while "k_L" is the lateral (in-plane) thermal conductivity (in the case of aluminum $k = k_L$). These definitions of the thermal conductances are the main differences between this model and the one introduced previously. A_1 and A_2 are shown in figure 5 and represent the surface area of the defect and the surface area of rest of the material, respectively. A_1 can be written as $A_1 = \pi R^2$ where R is the radius of the flat bottom hole, while A_2 will be assumed to tend to infinity ($A_2 \to \infty$). A_d is not shown explicitly in figure 5, but it represents the lateral cross sectional areas and can be expressed as $A_d = 2\pi R \cdot d$. The set of differential equations that define this problem are

$$\rho \cdot A_1 \cdot d \cdot c \cdot \frac{dT_1}{dt} = k_L \cdot \frac{A_L}{R} (T_2 - T_1)$$

$$\rho \cdot A_2 \cdot d \cdot c \cdot \frac{dT_2}{dt} = k_L \cdot \frac{A_L}{R} (T_1 - T_2) + k \cdot \frac{A_2}{d+h} (T_2' - T_2)$$

$$\rho \cdot A_2 \cdot h \cdot c \cdot \frac{dT_2'}{dt} = k \cdot \frac{A_2}{d+h} (T_2 - T_2') \tag{3}$$

where T_1, T_2, and T_2' are the temperatures of the different blocks as shown in figure 5. The boundary conditions of the problem are $T_1(t=0) = T_o$, $T_2(t=0) = T_o$, $T_2'(t=0) = 0$. This set of coupled differential equations can be easily solved in the limit when $A_2 \to \infty$. The contrast curve $\Delta T(t) = T_1(t) - T_2(t)$ obtained from it is

$$\Delta T(t) = \frac{Q}{\rho c \cdot d \cdot (1 - a + r)} \left(e^{-\frac{a}{d(d+h)} \frac{k}{\rho c} t} - e^{-\frac{1+r}{d(d+h)} \frac{k}{\rho c} t} \right) \tag{4}$$

where $a = \frac{k_L}{k} \frac{A_d}{A_1} \frac{d+h}{R}$ and $r = \frac{d}{h}$ (the variable "t = time" should not be confused with the parameter "t_o = panel thickness").

The maximum or peak thermal contrast can be calculated by differentiating equation 4, i.e.,

$$\Delta T_{max} = \frac{Q}{\rho c}\left(\frac{1}{d} - \frac{1}{t_o}\right) \cdot \left[\frac{a \cdot h}{t_o}\right]^{\frac{1}{\frac{t_o}{a \cdot h} - 1}} \tag{5}$$

which happens at a time give by

$$t_{max} = \frac{\rho c}{k}\frac{d \cdot t_o}{1 - a + r}\ln\frac{1 + r}{a} . \tag{6}$$

In comparing equations 1 and 5, it can be seen that the lateral heat flow effects can be grouped as a multiplicative factor to the main contrast relation equation 1.

ANALYSIS OF RESULTS FOR ALUMINUM PANEL

To understand the effects that the lateral flow of heat has on the peak thermal contrast ΔT_{max}, equation 5 needs to be studied further. If it is assumed that the material is isotropic, then the lateral and normal thermal conductivities will be the same. The parameter "a" can then be written as $a = A_d(d + h)/(A_1 R) = 2d(t_o - d)/R^2$, and the lateral heat flow contribution to the peak thermal contrast (the square bracket term in equation 5) can be simplified to

$$f_{lateral}(d) = \left[\frac{a \cdot h}{t_o}\right]^{\frac{1}{\frac{t_o}{a \cdot h} - 1}} = \left[\frac{2d \cdot (t_o - d)}{R^2}\right]^{\frac{1}{\frac{R^2}{2d(t_o - d)} - 1}} . \tag{7}$$

Figure 6 shows a graph of equation 7 for various hole diameters as a function of defect depth. From there it can be seen that, for flaws that are very close to the surface ($d \approx 0$) or for flaws that are very deep in the material ($d \approx t_o$), lateral heat flow effects tend to disappear in this model (or the lateral heat flow factor $f_{lateral}(d) \rightarrow 1$) and, as a result, the entire contribution to the peak thermal contrast will come from equation 1 (in which no lateral heat flow is assumed). This result can be explained as follows: In the limit $d \rightarrow 0$, the lateral conduction of heat will tend to zero because the lateral cross sectional area ($2\pi R \cdot d$) will become vanishingly small and therefore equation 1 is recovered. In the limit when $d \rightarrow t_o$, the lateral conduction of heat will tend to zero. In this limit, the temperature gradients will approach zero and therefore equation 1 is recovered. Finally, when $R \rightarrow \infty$, the lateral conduction of heat will again tend to zero because of the length over which the thermal energy has to travel is large and therefore equation 1 is recovered.
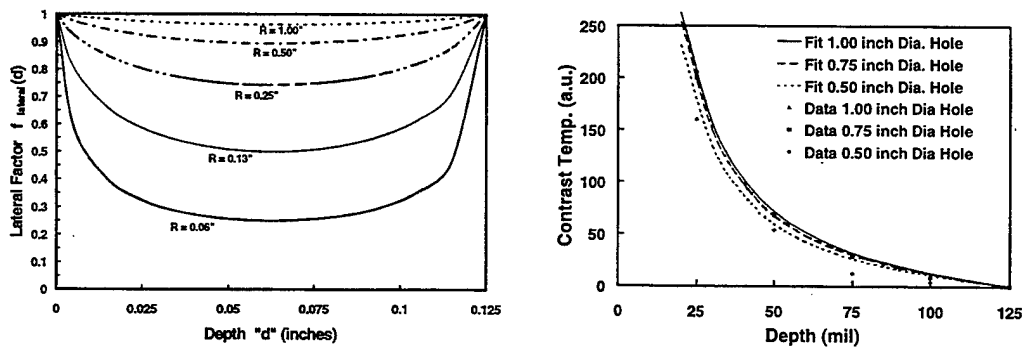

Figure 6: This figure shows the lateral heat flow factor (equation 7) as a function of the depth of the flaw for various hole radii.

7

Equation 5 was used to fit the experimental values of the peak contrast introduced at the beginning of the report. Figure 6 shows the result of the fits (lines) to the three sets of data points. Only one parameter (Q/ρc) was adjusted to fit all three data sets.

Equation 4 was used to fit all the experimental contrast curves. From figure 7, it can be seen that this simple model fits the experimental thermal contrast curves fairly well. The only parameter that was adjusted to fit all contrast curves was the thermal conductivity normalized to the specific heat-density "k/ρc". The best fit is for the data with 60% mass removal. The model does not fit the time period around the maximum for the 80% mass removal case.
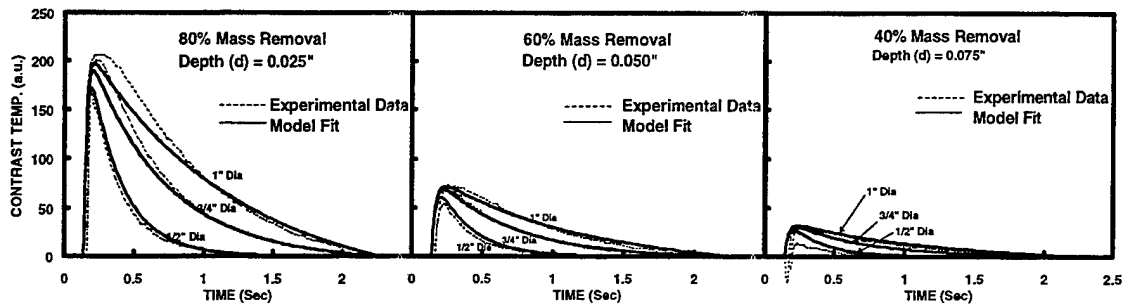

Figure 7: This figure shows the fit (solid lines) to the experimental contrast curve data (dotted lines). Each graph shows the contrast curves for three flat bottom holes at constant depth but with different diameter holes.

QUASI-ISOTROPIC MATERIALS

To validate the model further, a 1/8 in. thick graphite epoxy composite panel was fabricated with four 0.5 in. diameter flat bottom holes at various depths. The standard heat pulse experiment was performed on the sample. After careful analysis of the data, it was found that our simple model (equations 4, 5, and 6) was not able to adequately fit the data. Two factors are believed to be responsible for the discrepancies; a) the significantly larger thermal relaxation time of the Gr/Ep panel compared to the aluminum panel, and b) the larger in-plane thermal conductivity compared to the out-of-plane one. A new, more general model was developed. In this model (figure 8), it is assumed that the thickness of material over which the heat pulse is absorbed is a new variable defined by "p". A new set of differential equations can be written for this problem in the same fashion that the equations for the previous model (equation 3) were derived. The thermal conductances are defined in the same fashion as before (equation 2). A closed form solution can be found for the temporal dependence of the thermal contrast (not shown here because of its length). A closed form solution for the peak thermal contrast and for the time at which the peak thermal contrast happens has not been found. Figure 9 shows the results of this more general model. Some of the discrepancies in fit can be attributed to the choice of position of the reference point used to generate the background curve.
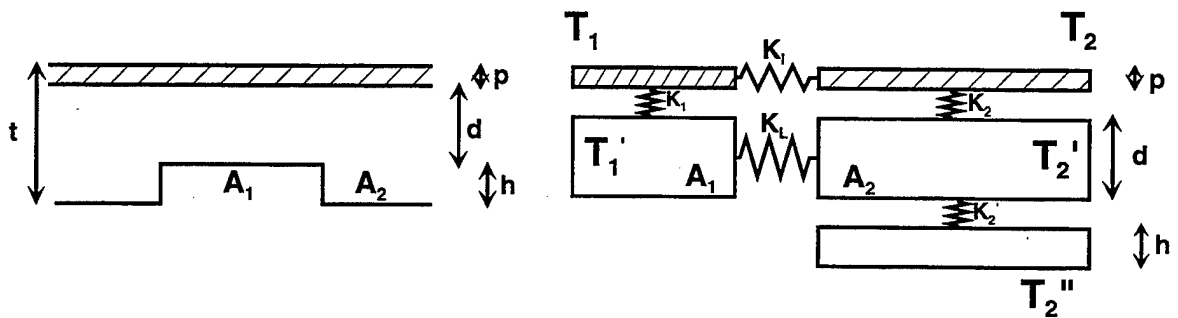
Figure 8: This figure shows the building blocks of our most general model.
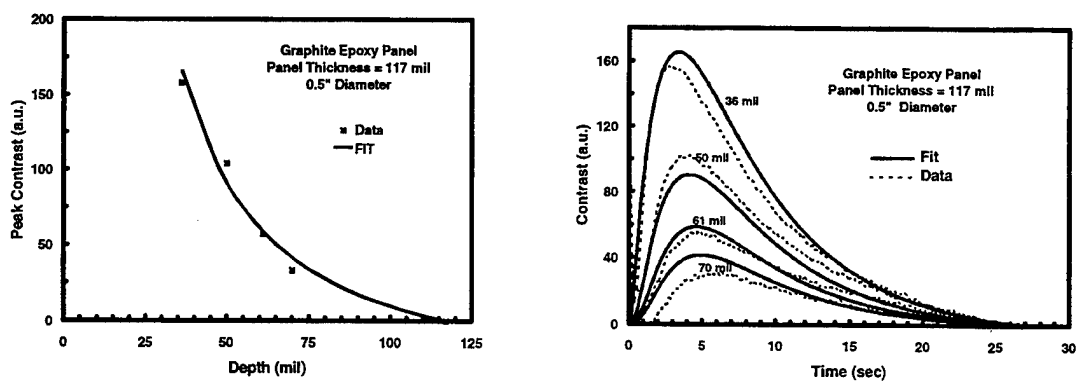

Figure 9: This figure shows the results of the fit of the new model to the four flat bottom holes in a graphite epoxy composite.

THIS PAGE INTENTIONALLY LEFT BLANK

CONCLUSIONS

Three simple models have been developed that describe the main features of thermal pulse analysis when applied to planar flaws. The last and most general of these models takes into account lateral heat conduction, anisotropic thermal conductivity, thickness, flaw size, density, and pulse duration. Equations 4, 5, and 6 of the second model provide a simple, yet accurate, description of the time dependence of the thermal contrast.

THIS PAGE INTENTIONALLY LEFT BLANK

REFERENCES

1. M.B. Saintey and D.P. Almond, "Mathematical Modelling of Transient Thermography and Defect Sizing", in *Review of Progress in QNDE*, Vol. 15, eds. D.O. Thompson and D.E. Chimenti, Plenum, NY, 1996, p. 503.

2. L.D. Favro, X. Han, P.K. Kuo, and R.L. Thomas, "Imaging the Early Time Behavior of Reflected Thermal Wave Pulses, in *Thermosense XVII*, SPIE, Vol. 2473, 1995, p. 162.

3. X.P.V. Maldague, "Nondestructive Evaluation of Materials by IR Thermography", Springer-Verlag, 1993, p. 29.

4. I.M. Perez, R. Santos, P.J. Kulowitch, M.J. Ryan, "Calorimetric Modeling of Thermographic Data", in *Thermosense XX*, SPIE, Vol. 3361, 1998, p. 75.

THIS PAGE INTENTIONALLY LEFT BLANK

DISTRIBUTION:

ONR Arlington, VA	(1)
USAF Research Laboratory (AFRL/MLLP) Wright Patterson AFB, OH	(2)
NASA LaRC NDE Sciences Branch, Hampton, VA	(1)
National Defence Headquarters (H/AVRD) Ottawa, Ontario, Canada	(1)
Army Materials Laboratory (AMSRL-WM-MD)	(1)
NAVSURFWARCEN Carderock Division (Welding and NDE Branch)	(2)
NRL Washington, DC	(2)
NAVAVNDEPOT Cherry Point, NC (4.3.4)	(1)
NAVAVNDEPOT Jacksonville, FL (4.3.4)	(1)
NAVAVNDEPOT San Diego, CA (4.3.4)	(1)
NAVAIRSYSCOM (AIR-4.3.4.2)	(23)
NAVAIRWARCENACDIV Patuxent River, MD (Technical Publishing Team)	(1)
DTIC	(1)